References

[1] Rasmussen, R. E. H., "Über die Strömungen von Gasen in engen Kanalen," Ann. Physik **5**, 29 (1937).

[2] Cercignani, C., "Plane Poiseuille flow and Knudsen minimum effect," 3rd International Symposium on Rarefied Gas Dynamics, Paris (June 1962).

[3] DeMarcus, W. C., "The problem of Knudsen flow," U. S. Atomic Energy Commission Rept. K-1302, ORGDP (1956).

[4] Pao, Y. P., "Some results for plane Poiseuille flow of rarefied gases," Rept. 619, Dept. Aeronaut. Eng., Princeton Univ. (1962).

Nonequilibrium Plasma Characteristics in Hypersonic One-Dimensional Flow

FRED MEYER,* W. K. H. KRESSNER,† AND J. R. STEFFEY‡

Boeing Company, Seattle, Wash.

FOR the case of one-dimensional steady flow in a streamtube of constant cross section with negligible viscosity and diffusion, the kinetic and gasdynamical flow equations have been combined in a single set of differential equations describing the composition and flow of a system of reacting gases. A rather complete chemical model considering 10 reversible reactions is used together with reaction rates published by Teare, Kivel, Hammerling, et al.[1] Investigation of the chemical rate equation with a given set of rate constants leads to the determination of temperature, air-density, and particle-concentration histories behind the shock front.

The following set of equations comprises the heart of the program:

$$\frac{1}{\rho}\frac{d\rho}{dx} + \frac{1}{v}\frac{dv}{dx} = 0 \tag{1}$$

$$\frac{\rho v}{p}\frac{dv}{dx} + \frac{1}{p}\frac{dp}{dx} = 0 \tag{2}$$

$$v\frac{dv}{dx} + \frac{dh}{dx} = 0 \tag{3}$$

$$\frac{1}{\rho}\frac{d\rho}{dx} - \frac{1}{p}\frac{dp}{dx} + \frac{1}{T}\frac{dT}{dx} - \frac{1}{\overline{W}}\frac{d\overline{W}}{dx} = 0 \tag{4}$$

$$\frac{1}{\overline{W}}\frac{d\overline{W}}{dx} = -\frac{\overline{W}\Sigma_i\gamma_i}{\rho v} \tag{5}$$

$$\frac{dh}{dx} - \bar{c}_p\frac{dT}{dx} = \frac{\Sigma_i H_i\gamma_i}{\rho v} \tag{6}$$

The first three equations are the differential forms of the overall equations of continuity, conservation of momentum, and conservation of energy, respectively. Equation (4) is the differential form of the gas law or thermal equation of state, where

$$\overline{W} = \Sigma_i(Y_i/W_i)^{-1} = \Sigma_i W_i r_i/\Sigma_i r_i$$

is the average molecular weight of the mixture of the ith species, W_i is the gram molecular weight of the ith species, $r_i = \rho(Y_i/W_i)$ is the concentration in moles per unit volume of the ith species, and Y_i/W_i is the number of moles of species i per gram of original air.

The fifth equation is the differential form of $\overline{W} = \Sigma_i(Y_i/W_i)^{-1}$ after application of the equations of continuity for the individual species in the flowing mixture, neglecting diffusion:

$$\rho v(dY_i/dx) = W_i\gamma_i$$

where γ_i is the rate at which species i is produced per unit time-per unit volume and is computed from the postulated chemical mechanism according to the standard methods of chemical kinetics.

The last equation is the differential form of the enthalpy of the mixture of gases, where $\bar{c}_p = \Sigma_i Y_i c_{pi}$ is the average heat capacity at constant pressure, and H_i is the molar heat capacity of the ith species. This assumes that $[(\partial h_i/\partial p)]_T = 0$, a good approximation for the high temperatures and low pressures corresponding to re-entry conditions. The thermodynamic functions required for each species were computed from its partition function using the approximations developed by Hochstim for these species.[2]

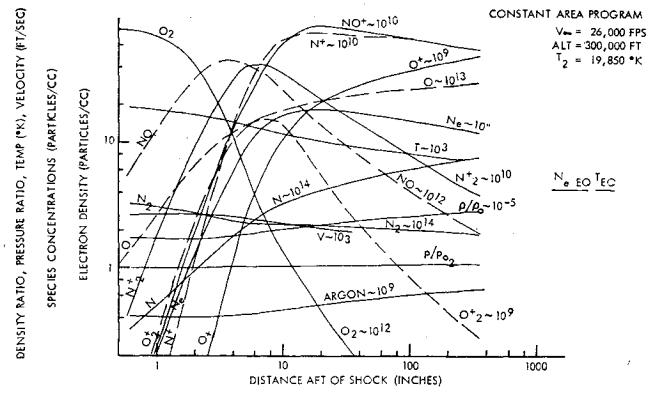

Fig. 1 Species and flow-property histories aft of normal shock

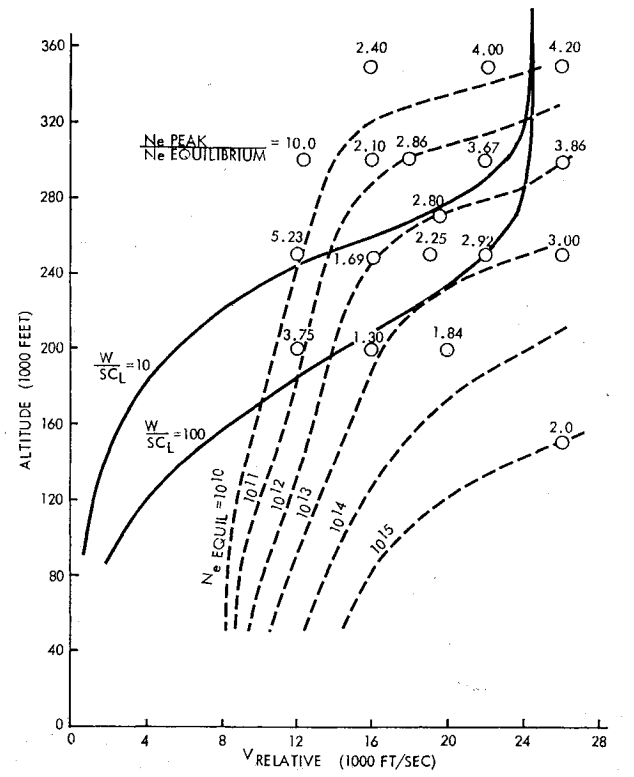

Fig. 2 Peak electron-density overshoots aft of normal shock

Received January 14, 1963.

* Research Specialist, Aerospace Division.

† Research Engineer, Aerospace Division.

‡ Associate Engineer, Aerospace Division.

Table 1 Reaction mechanism for shocked air[1]

Index, j	Reaction	Exothermic Rate Constant $k_j^{(r)}$, or $k_{M,j}^{(r)}$ for catalyzed reactions, with catalyst M. Here, $k_{M,j}^{(r)} \equiv \mu_{M,j} k_j^{(r)}$, $k_j^{(r)} = k_{A,j}^{(r)}$		
		$k_j^{(r)}$	Catalyst M	Cat. Eff. Factor $\mu_{M,j}$
1	$N_2 + M + 9.8$ e.v. $\rightleftharpoons N + N + M$	$\frac{10^{15}}{6}\left(\frac{T}{4500}\right)^{-3/2}$ $cm^6\ moles^{-2} sec^{-1}$	N_2 N A, O_2, O NO	3 15 1
2	$O_2 + M + 5.1$ e.v. $\rightleftharpoons O + O + M$	$\frac{2 \times 10^{14}}{3}\left(\frac{T}{4500}\right)^{-3/2}$ $cm^6 moles^{-2} sec^{-1}$	O_2 O A, N_2, N, NO	3 15 1
3	$NO + M + 6.5$ e.v. $\rightleftharpoons N + O + M$	$\frac{10^{15}}{3}\left(\frac{T}{4500}\right)^{-3/2}$ $cm^6 moles^{-2} sec^{-1}$	N_2, N, O_2, O NO A	6 6 1
4	$NO + O + 1.4$ e.v. $\rightleftharpoons N + O_2$	$10^{12} T^{1/2} \exp(-3120/T)$ $cm^3 mole^{-1} sec^{-1}$		
5	$N_2 + O + 3.3$ e.v. $\rightleftharpoons NO + N$	1.3×10^{13}	$cm^3 mole^{-1} sec^{-1}$	
6	$N + O + 2.8$ e.v. $\rightleftharpoons NO^+ + e^-$	$3 \times 10^{-3} T^{-3/2}$	cm^3 molecule^{-1} sec^{-1}	
7	$N^* + N + (5.8$ e.v.$) \rightleftharpoons N_2^+ + e^-$	$1.6 \times 10^{-2} T^{-3/2}$	cm^3 molecule^{-1} sec^{-1}	
8	$O^* + O + (6.9$ e.v.$) \rightleftharpoons O_2^+ + e^-$	$3.2 \times 10^{-3} T^{-3/2}$	cm^3 molecule^{-1} sec^{-1}	
9	$N_2 + N^+ + 1.0$ e.v. $\rightleftharpoons N_2^+ + N$	$1.3 \times 10^{-12} T^{-1/2}$	cm^3 molecule^{-1} sec^{-1}	
10	$O_2^+ + O + 1.6$ e.v. $\rightleftharpoons O_2 + O^+$	$1.3 \times 10^{-12} T^{1/2}$	cm^3 molecule^{-1} sec^{-1}	

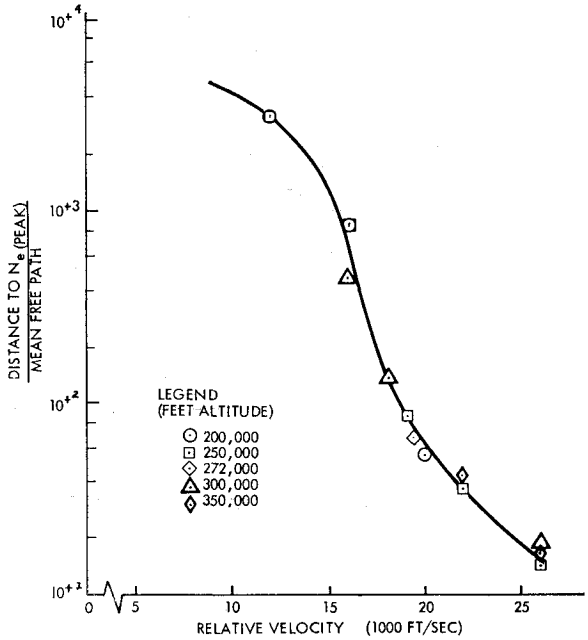

Fig. 3 Distance to electron density peaks

The 10 reactions employed in the program are presented with the corresponding reaction-rate constants for the reverse reactions in Table 1. For the first three reactions, the known catalysts and their effect upon the speed of the reaction are presented. The effect of a third body, required for the recombination reaction, in catalyzing the reaction is accounted for conveniently by the catalytic efficiency factor shown in column four. The reaction-rate constants used were obtained from Ref. 1.

Figure 1 shows typical program results of species-concentration as well as flow-property histories for a velocity of 26,000 fps and an altitude of 300,000 ft. Of interest are the peak values of "overshoots" and the location of these peaks exhibited by several species—in particular, the electron density. (The program was developed originally to assess real-gas effects on communications during hypersonic reentry; hence the electron-density distribution was of major concern.) Ratios of peak to equilibrium electron density have been computed for several altitudes and velocities and are shown in Fig. 2. Typical glide trajectories for values of $W/SC_L = 10$ and 100 are superimposed. Within the glide corridor shown and above 200,000 ft, it appears that the nonequilibrium effects are relatively small, as evidenced by ratios of $N_{e\ peak}/N_{e\ equil} < 5.0$.

Distances from the shock front to peak electron density were computed for a variety of velocity-altitude conditions and have been found to correlate reasonably well when nondimensionalized with respect to the mean free path in the undisturbed air for any one velocity, as shown in Fig. 3.

References

[1] Wray, K., Teare, J. D., Kivel, B., and Hammerling, P., "Relaxation processes and reaction rates behind shock fronts in air and component gases," Research Rept. 83, Avco-Everett Research Lab. (December 1959).

[2] Hochstim, A. R., "Approximations to high temperature thermodynamics of air in closed form," Western State Meeting of the Combustion Institute, Los Angeles, Calif. (November 2, 1959).